29th Congress of the International Council of the Aeronautical Sciences
St. Petersburg, Russia; September 7-12, 2014

DYNAMIC NOTCH FILTERING CONTROL FOR FAULT-TOLERANT ACTUATORS OF FLY-BY-WIRE HELICOPTERS

Di Rito G. *, Galatolo R. *, Denti E. * and Schettini F. *
*Università di Pisa, Dipartimento di Ingegneria Civile e Industriale - Sez. Aerospaziale

Keywords: *fly-by wire helicopter, fault-tolerant actuator, control design, jump resonance*

Abstract

The paper deals with the control design of a fault-tolerant actuator for fly-by-wire helicopters, capable of compensating both failure effects and jump resonance phenomena.

The study, focused on the performance analysis in case of servovalve coil faults, points out that a standard reconfiguration based on demand amplification can imply jump resonances. The proposed strategy eliminates the problem by correlating the jump frequency to the system characteristics, and by inserting a dynamic notch filter in the actuator closed-loop control.

1 Introduction

Full-authority Fly-By-Wire Flight Control Systems (FBW/FCS) are nowadays a standard technology solution for advanced aircraft and rotorcraft. To provide the adequate level of safety, the actuators for the primary flight controls are designed to be fault-tolerant equipments, so that they must be able to appropriately operate in the event of one or more failures [1] [2]. The performance analysis of a fault-tolerant actuator thus plays an important role during the verification and validation process of a FBW/FCS, especially during on-ground testing [3]. The effects of equipment nonlinearities (e.g. saturations, dead bands, freeplays, etc.) should be actually pointed out and compensated well before the first flight. In particular, if the actuator is commanded with large amplitude demands, saturation phenomena (e.g. current or voltage limits, valve port limit for hydraulic actuators) can be encountered, and the response can exhibit large increases of phase lag over a very narrow frequency band. This is described by the term “jump resonance”, although the gain peak associated to the sharp phase variation can be moderated or lacking [4] [5]. Saturation conditions can be reached during extreme manoeuvres, and the additional phase lag caused by a jump resonance can lead to severe temporary reduction of vehicle stability margins, with consequent potential handling difficulties. As outlined in [4], the jump resonance reduces as demand amplitude increases, and the phenomenon can become critical if fault-tolerant actuators with active redundancies are concerned. Actually, after a failure, the actuator performance is typically maintained by isolating the failed element and by reassigning the function to the remaining ones (i.e. by increasing the command in the active lanes) [6], and jump resonances can occur within the frequency range of interest for flight control operations. The phenomenon is relevant for all fly-by-wire flight control applications, but it must be regarded with particular care for the helicopter case, since the interaction between oscillating loads and actuator jump resonances can bring on accentuate performance degradation and even safety issues (e.g. aeroservoelastic concerns).

This work deals with the development of a reconfiguration strategy of the closed-loop control of a fault-tolerant hydraulic actuator for fly-by-wire helicopters, capable of compensating both failure effects and jump resonance phenomena. The paper is organized into three main sections. Firstly, the reference actuator is described in terms of fault-tolerant architecture and closed-loop control scheme. In the second part, the actuator dynamics in case of current saturation is analysed, by identifying the relationship between the jump resonance and the system dynamic characteristics. Finally, two control reconfiguration strategies are compared: a standard one based on command amplification, and an alternative one, developed by the authors, in which a dynamic notch filter located at the jump resonance frequency is applied in the servovalve loop. The actuator dynamics is characterised in terms of both servovalve and actuator frequency responses by means of an experimentally-validated Matlab-Simulink model developed by the authors [7], highlighting the effectiveness of the approach.

2 Equipment description

2.1 Fault-tolerant actuator layout

The reference actuator is characterised by a complex redundant architecture that allows the equipment to maintain its functionality even after one or more failures. It is essentially composed of (Fig. 1):

- a tandem hydraulic cylinder
- an eight-way rotary valve (Fig. 2.a), driven by a limited-angle DC brushless motor with four independent coils (Fig. 2.b)
- four LVDT transducers for the actuator position sensing
- four RVDT transducers for the valve rotation sensing.

The actuator is interfaced with two independent hydraulic power supplies and four Flight Control Computers (FCCs). Each FCC is equipped with a quadruple PWM electronics (for driving one of the servovalve motor coil of each of the four helicopter primary actuators), and with a quadruple FPGA electronics (for implementing the actuator closed-loop controls). In normal operative conditions (i.e. no failures), three control lanes of the actuator are active, while the fourth one is in “stand-by”. The equipment can thus tolerate up to three servovalve coil faults, provided that an appropriate control reconfiguration is applied.

2.2 Closed-loop controls

The actuator closed-loop control[1] is composed of three nested digital loops, on servovalve motor currents, servovalve rotation and ram position respectively (Fig. 3).

2.2.1 Current control

The servovalve motor current control outputs the target voltage for the PWM coil drive ($V_{c\text{dem}}$) by processing the error between the coil current demand ($i_{c\text{dem}}$) and the sensed coil current (i_c), via a proportional regulator Eq. (1).

$$V_{c\,\text{dem}} = K_{iP}(i_{c\,\text{dem}} - i_c) \tag{1}$$

The control output ($V_{c\text{dem}}$) is also processed by a saturation/anti-windup block to avoid that the demand voltage exceeds the supply voltage.

2.2.2 Servovalve control

The servovalve control outputs the coil current demand ($i_{c\text{dem}}$) by processing the error between the spool rotation demand ($\theta_{v\text{dem}}$) and the sensed spool rotation (θ_v), and providing a proportional action (gain K_{vP}) and a speed-proportional stability augmentation action (gain K_{vD}), Eq. (2).

$$i_{c\,\text{dem}} = K_{vP}(\theta_{v\,\text{dem}} - \theta_v) - K_{vD}\,\dot{\theta}_v \tag{2}$$

The control output ($i_{c\text{dem}}$) is also processed by a saturation/anti-windup block, to avoid that the demand current exceeds the current limit for the motor coil.

2.2.3 Ram control

The ram position control finally outputs the spool rotation demand ($\theta_{v\text{dem}}$) by processing the error between the ram position demand ($x_{a\text{dem}}$) and the sensed ram position (x_a), via a proportional regulator, Eq. (3).

$$\theta_{v\,\text{dem}} = K_{rP}(x_{a\,\text{dem}} - x_a) \tag{3}$$

The control output ($\theta_{v\text{dem}}$) is also processed by a saturation/anti-windup block to avoid that the spool rotation demand exceeds the port width limit.

[1] A quite simple structure of the regulators is here assumed, to better focus the discussion on the system dynamics analysis.

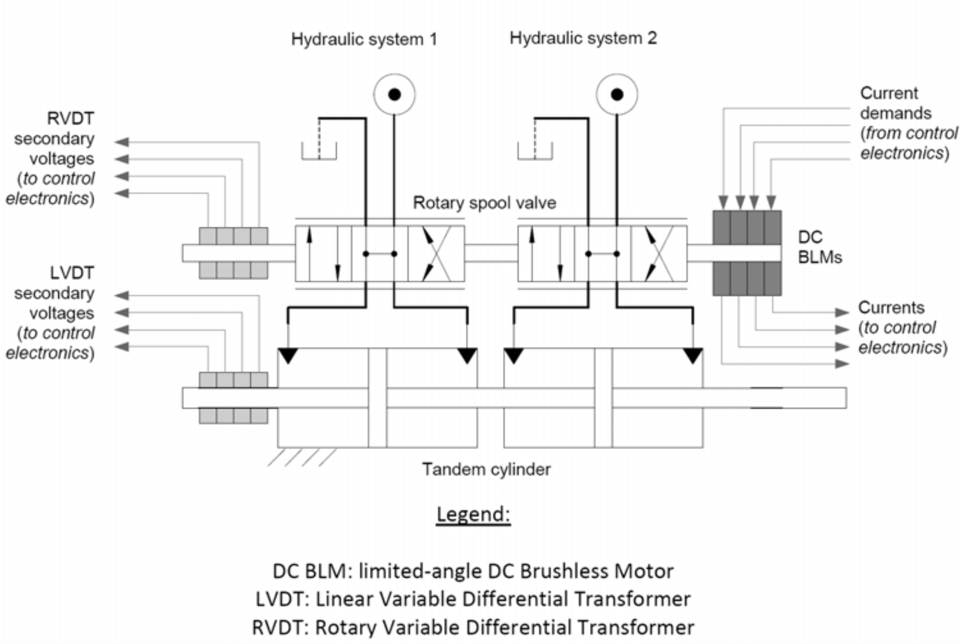

Fig. 1. Fault-tolerant actuator for fly-by-wire helicopter.

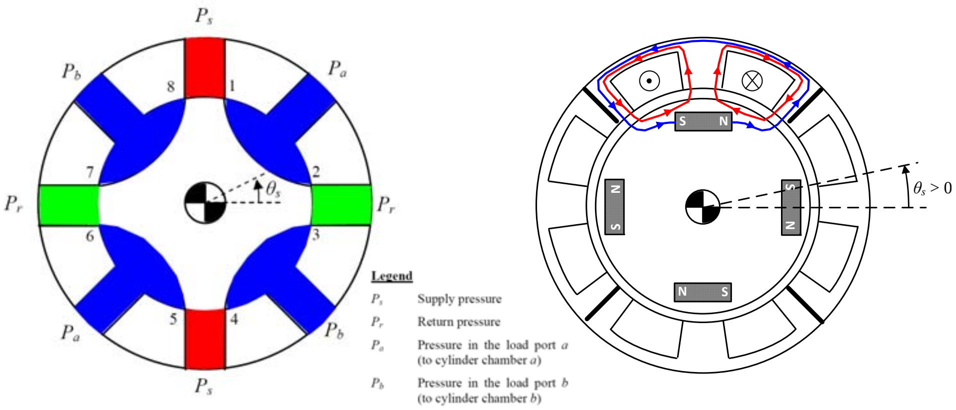

Fig. 2. Actuator servovalve: (a) single unit of the rotary valve; (b) limited-angle brushless motor.

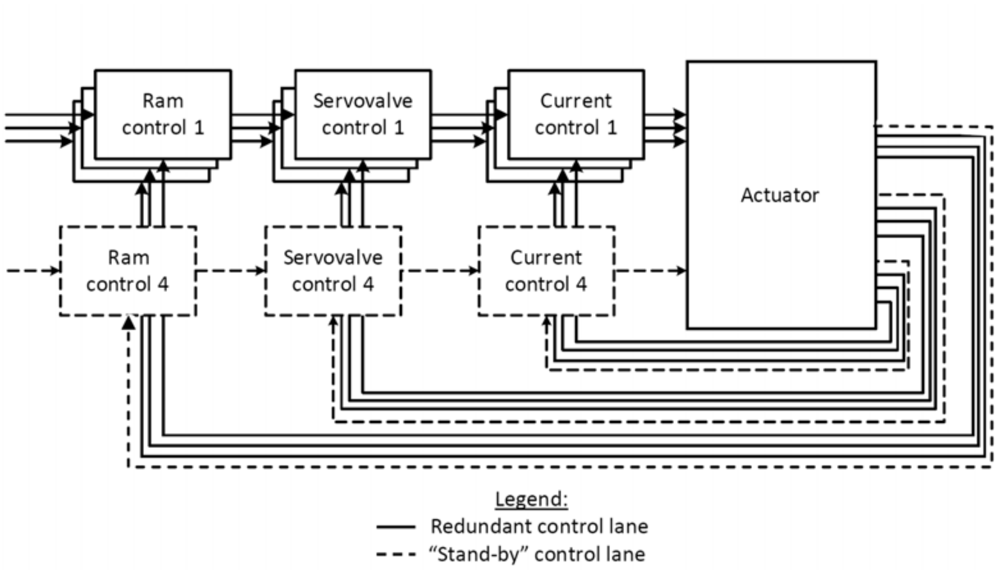

Fig. 3. Actuator closed-loop control scheme.

3 Actuator dynamics in case of current saturation

3.1 System modelling

The understanding of the actuator behaviour in case of current saturation is strictly related to the analysis of the servovalve dynamics in these conditions. A simplified relationship between the spool shaft rotation (θ_v) and the current in a motor coil (i_c) is provided by Eq. (4),

$$J_v \ddot{\theta}_v = n_c K_{t1} i_c \qquad (4)$$

where J_v is the spool shaft inertia, n_c is the number of active coils and K_{t1} is the motor torque constant related to a single magnet-coil coupling.

Provided that the current control is capable of a very rapid tracking of the current demand signal ($i_{c\,\mathrm{dem}}$), a good approximation of the coil current dynamics is given by Eq. (5)[2]

$$i_c \approx \begin{cases} i_{c\,\max} & \left|i_{c\,\mathrm{dem}}\right| > i_{c\,\max} \\ i_{c\,\mathrm{dem}} & \left|i_{c\,\mathrm{dem}}\right| \le i_{c\,\max} \end{cases} \qquad (5)$$

where $i_{c\,\max}$ is the coil current limit, and $i_{c\,\mathrm{dem}}$ is given by Eq. (2).

By using Eq. (5) into Eq. (4), and by applying the Laplace transform, the servovalve rotation transfer functions related to both nominal conditions (no saturation) and in case of current saturation can be obtained, Eq. (6),

$$\theta_v(s) = \begin{cases} \dfrac{n_c K_{t1} i_{c\,\max}}{J_v s^2} & \left|i_{c\,\mathrm{dem}}\right| > i_{c\,\max} \\ \dfrac{a_{v0}}{s^2 + a_{v1} s + a_{v0}} \theta_{v\mathrm{dem}}(s) & \left|i_{c\,\mathrm{dem}}\right| \le i_{c\,\max} \end{cases} \qquad (6)$$

where $a_{v0} = \dfrac{n_c K_{t1} K_{vP}}{J_v}$ and $a_{v1} = \dfrac{n_c K_{t1} K_{vD}}{J_v}$.

A rough (but useful for basic physical interpretations) approximation of the actuator dynamics can be finally obtained by combining Eq. (6) with Eqs. (7)-(8),

$$A_a \dot{x}_a = K_q \theta_v \qquad (7)$$

$$\theta_{v\,\mathrm{dem}} = K_{rP}(x_{a\,\mathrm{dem}} - x_a) \qquad (8)$$

where K_q is the servovalve flow gain, A_a is the actuator pushing area, and K_{rP} is the proportional gain of the ram control (Eq. (3)). The actuator position transfer functions related to both nominal conditions and in case of current saturation are thus given by Eq. (9),

$$x_a(s) = \begin{cases} \dfrac{K_q n_c K_{t1} i_{c\,\max}}{A_a J_v s^3} & \left|i_{c\,\mathrm{dem}}\right| > i_{c\,\max} \\ \dfrac{a_{r0}}{s^3 + a_{r2} s^2 + a_{r1} s + a_{r0}} x_{a\mathrm{dem}}(s) & \left|i_{c\,\mathrm{dem}}\right| \le i_{c\,\max} \end{cases} \qquad (9)$$

where $a_{r0} = \dfrac{K_q n_c K_{t1} K_{vP} K_{rP}}{J_v A_a}$, $a_{r1} = a_{v0}$ and $a_{r2} = a_{v1}$. Equation (9) points out that, if no current saturation occurs, the actuator essentially responds to the position demand as a third-order system with zero steady-state error at step input. On the other hand, if current saturation occurs, the actuator behaves as a third-order system with three poles at the origin.

3.2 Characterisation of the jump resonance phenomenon

By referring to Eq. (2) and Eq. (5), the condition for current saturation is:

$$\left|K_{vP}(\theta_{v\,\mathrm{dem}} - \theta_v) - K_{vD}\dot{\theta}_v\right| \ge i_{c\,\max} \qquad (10)$$

If we apply the Laplace transform and substitute into Eq. (10) the servovalve rotation transfer function at marginal saturation condition (Eq. (6) with $|i_{c\mathrm{dem}}| = i_{c\,\max}$), the current saturation condition in the frequency domain can be obtained, Eq. (11),

$$\left|G_v(s)\right| \ge L_{sat} \qquad (11)$$

where

$$G_v(s) = \frac{n_c K_{t1} K_{vP} s^2}{J_v s^2 + n_c K_{t1} K_{vD} s + n_c K_{t1} K_{vP}} \qquad (12)$$

[2] Considering the values of current closed-loop bandwidth for these applications, the simplification is acceptable for frequencies up to 100 Hz.

$$L_{sat} = \frac{n_c K_{t1} i_{c\,\max}}{J_v \left|\theta_{v\,\mathrm{dem}}\right|} \qquad (13)$$

The jump resonance frequency (ω_{jr}) in case of current saturation can be thus defined by means of Eq. (14),

$$\omega_{jr} = \min\left(|s|, \left|G_v(s)\right| \geq L_{sat}\right) \qquad (14)$$

In practical applications, the servovalve control is designed to obtain a well-damped response to the spool rotation demand, so it is typically expected that the amplitude response of the transfer function $G_v(s)$ exhibits no overshoot with respect to frequency. Under this assumption, a jump resonance can exist only if

$$G_{v\,\infty} = \lim_{s\to\infty} G_v(s) = \frac{n_c K_{t1} K_{vP}}{J_v} \geq L_{sat} \qquad (15)$$

By substituting Eq. (13) with Eq. (15), we obtain that the jump resonance existence essentially depends on the servovalve demand amplitude ($|\theta_{v\,\mathrm{dem}}|$) and on the proportional gain of the servovalve control (K_{vP}), Eq. (16).

$$\left|\theta_{v\,\mathrm{dem}}\right| \geq \frac{i_{c\,\max}}{K_{vP}} \qquad (16)$$

As previously stated, the jump resonance frequency can be calculated via Eq. (14), but a practical (and conservative) estimation can be obtained by assuming that the current saturation condition occurs in the low-frequency domain, Eq. (17),

$$\left|G_{v0}(s)\right| \geq L_{sat} \qquad (17)$$

where

$$G_{v0}(s) = \lim_{s\to 0} G_v(s) = s^2 \qquad (18)$$

By combining Eq. (13) with Eqs. (17)-(18), we finally obtain the following approximation of the jump resonance frequency:

$$\tilde{\omega}_{jr} = \sqrt{\frac{n_c K_{t1} i_{c\,\max}}{J_v \left|\theta_{v\,\mathrm{dem}}\right|}} = \sqrt{n_c \frac{\left|\ddot{\theta}_{v\,1\,\max}\right|}{\left|\theta_{v\,\mathrm{dem}}\right|}} \qquad (19)$$

Equation (19) points out that, once defined the maximum servovalve angular acceleration at single coil operation ($\left|\ddot{\theta}_{v\,1\,\max}\right|$, imposed by basic characteristics as J_v , $i_{c\max}$ and K_{t1}), the jump resonance frequency is proportional to the square root of the number of active coils, and inversely proportional to the square root of the valve demand amplitude. The plot in Fig. 4 reports an example of amplitude response of the transfer function $G_v(s)$ together with two values of the quantity L_{sat}, related to valve demand amplitudes that imply or not current saturation.

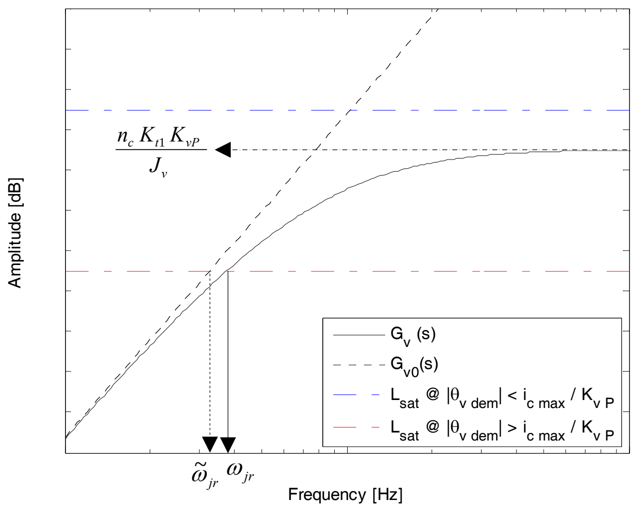

Fig. 4. Jump resonance frequency estimation.

4 Actuator control reconfiguration strategies

4.1 Standard reconfiguration

The most common reconfiguration strategy applied in fault-tolerant actuators is based on command amplification, which results from the isolation of the failed element and the reassignment of its function to the remaining active elements. In case of servovalve coil failures, this strategy implies the following variation of the servovalve control gains:

$$K_{vP} = \frac{3}{n_c} K_{vP3} \qquad (20)$$

$$K_{vD} = \frac{3}{n_c} K_{vD3} \qquad (21)$$

where K_{vP3} and K_{vD3} are the proportional and stability augmentation gains of the servovalve control in normal operative condition (no failures, 3 active coils).

4.2 Reconfiguration with Dynamic Notch Filter (DNF) compensation

The proposed reconfiguration strategy aims to compensate both failure effects and jump resonance phenomena. The basic idea is to insert a Dynamic Notch Filter (DNF) in the feed-forward path of the servovalve rotation control, in order to reduce the current demand amplitude in that critical frequency range, Eq. (22).

$$i_{c\,\text{dem}} = G_{DNF}(s)\,\{K_{vP}[\theta_{v\,\text{dem}} - \theta_v] - K_{vD}\, s\,\theta_v\} \quad (22)$$

In particular, the DNF pulsation is located at the jump resonance frequency estimated by Eq. (19), while its damping factors are assumed constant parameters, Eq. (23).

$$G_{DNF}(s) = \frac{s^2 + 2\zeta_{DNF\,n}\,\tilde{\omega}_{jr}\, s + \tilde{\omega}_{jr}^{\,2}}{s^2 + 2\zeta_{DNF\,d}\,\tilde{\omega}_{jr}\, s + \tilde{\omega}_{jr}^{\,2}} \quad (23)$$

Concerning the servovalve control gains, the reconfiguration in case of coil failures is the one described at section 4.1, Eqs. (20)-(21).

4.3 Actuator performance analysis

To evaluate the effectiveness of the approach, the two control reconfiguration strategies have been implemented into an experimentally-validated Matlab-Simulink model of the fault-tolerant actuator developed by the authors [7]. The actuator dynamics has been characterised in terms of both servovalve and actuator frequency responses, with reference to the normal operative condition and with failures.

Fig. 5 and Fig. 6 report the results of the performance analysis carried out for the servovalve, and they allow to clearly verify the effectiveness of the proposed technique.

In the normal operative condition, if no DNF compensation is applied, the servovalve response exhibits jump resonance phenomena above 40% valve demands, with dramatic increases of gain and phase lag. As an example, at 50% valve demand, the jump resonance occurs at 70 Hz, with an amplitude response variation of about 4 dB and a phase lag at about -180° (confirming the relationship between the phenomenon and the current saturation, Eq. (6)). On the other hand, if the DNF compensation is used, the jump resonance effects are shifted to higher frequencies and almost cancelled (some slight hints can be observed at about 85 Hz). The servovalve dynamics behaves very regularly, also exhibiting a good linearity (the response variation with the demand amplitude is very limited).

In the worst-case electrical condition (1 active coil), the usefulness of the DNF compensation is even more convincing, as a result of the command amplification induced by the reconfiguration of the servovalve control. Without the DNF, the servovalve exhibits jump resonances above 25% valve demands, with frequencies ranging from 40 to 50 Hz, and with remarkable response amplification (up to 1 dB). If the DNF is inserted, the jump resonance frequencies are again shifted to high-frequency range[3], and no gain peaks are present.

The benefits of the DNF compensation are also significant at actuator level, as shown by the position frequency responses of Fig. 7 and Fig. 8. The effectiveness is particularly significant in case of 1 coil operation: without DNF compensation, the response at 2% position demand exhibits a jump resonance at 35 Hz, with +6 dB gain increase and a phase lag that abruptly approaches -270° (confirming again that the phenomenon is related to the current saturation, Eq. (9)). If the DNF compensation is applied, the jump resonance frequency is shifted to 45 Hz and its effects are strongly reduced (the gain increase is lower than +3 dB).

It must be emphasized that the capability of the proposed technique of minimising and sometimes cancelling jump resonances in the actuator response is interesting for all fly-by-wire flight control applications, since the phenomenon is typically associated with a reduction of stability margins or unexpected aeroservoelastic interactions. This is even more relevant for the helicopter case, where the interaction between oscillating loads and actuator jump resonances can bring on performance degradation and even safety concerns [4].

[3] As an example, at 25% valve demand, the jump resonance frequency is moved to 70 Hz.

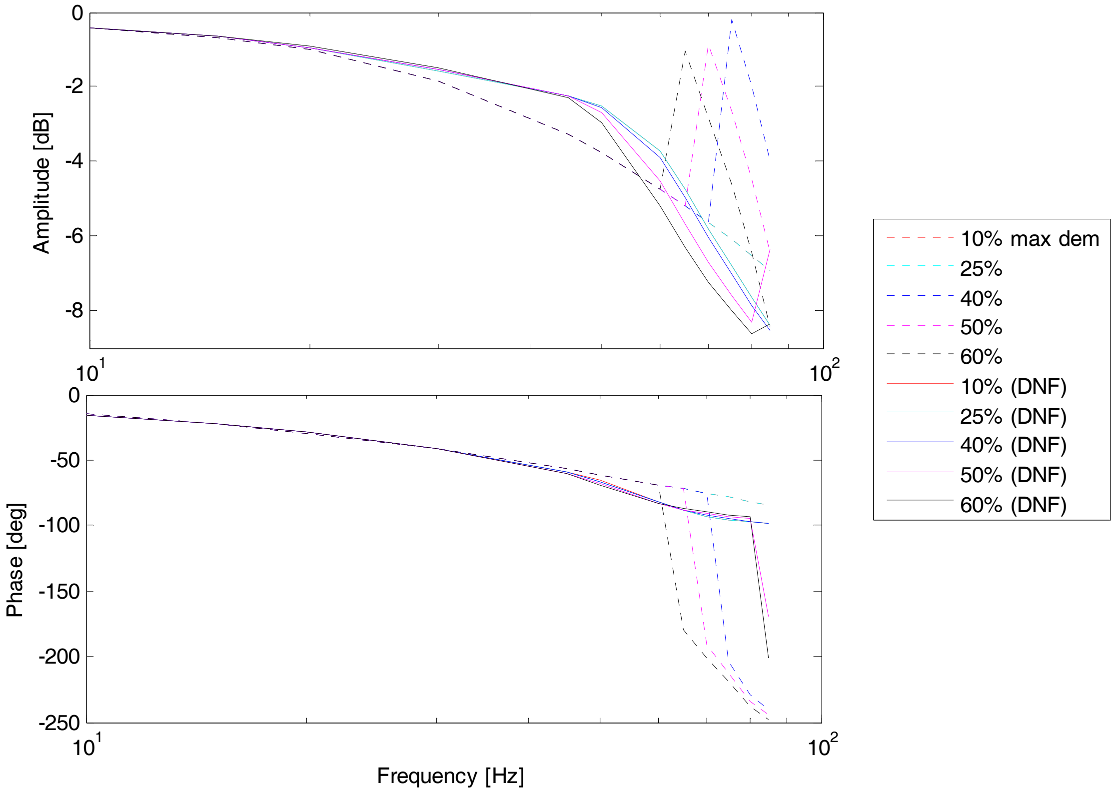

Fig. 5. Effects of the DNF on the servovalve closed-loop dynamics (3 active coils).

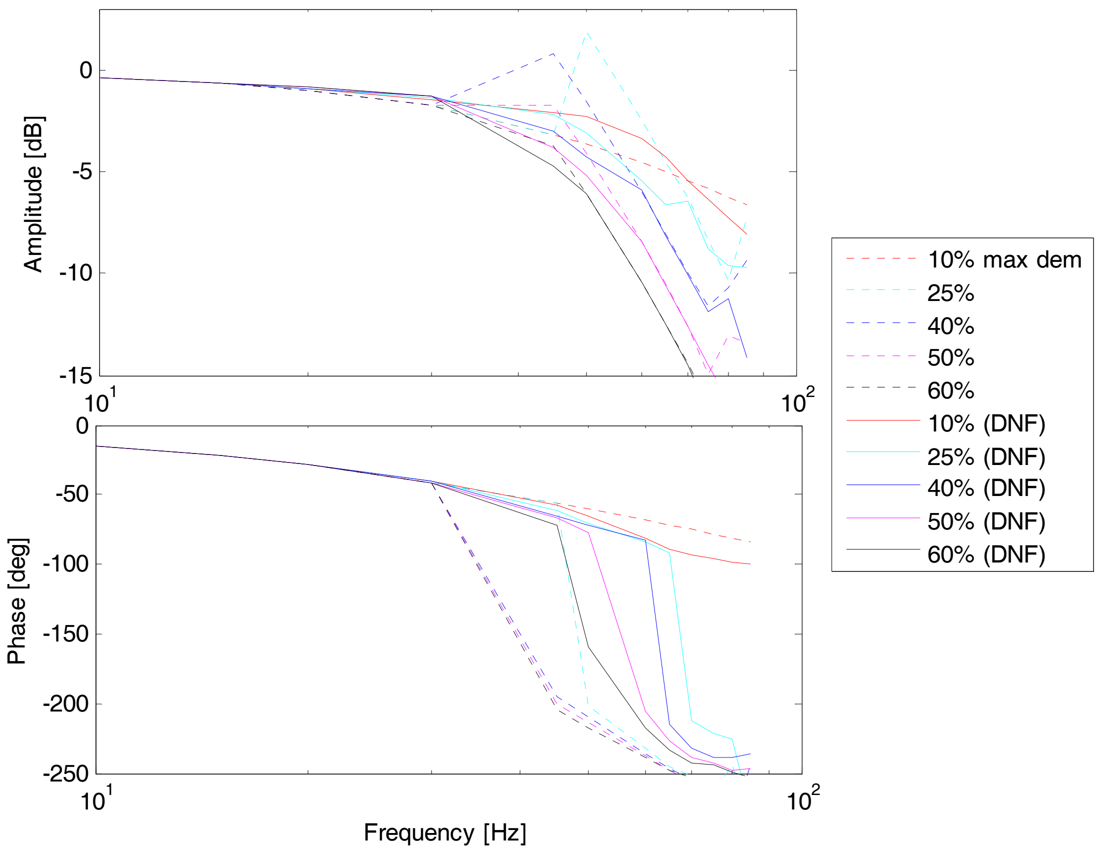

Fig. 6. Effects of the DNF on the servovalve closed-loop dynamics (1 active coil).

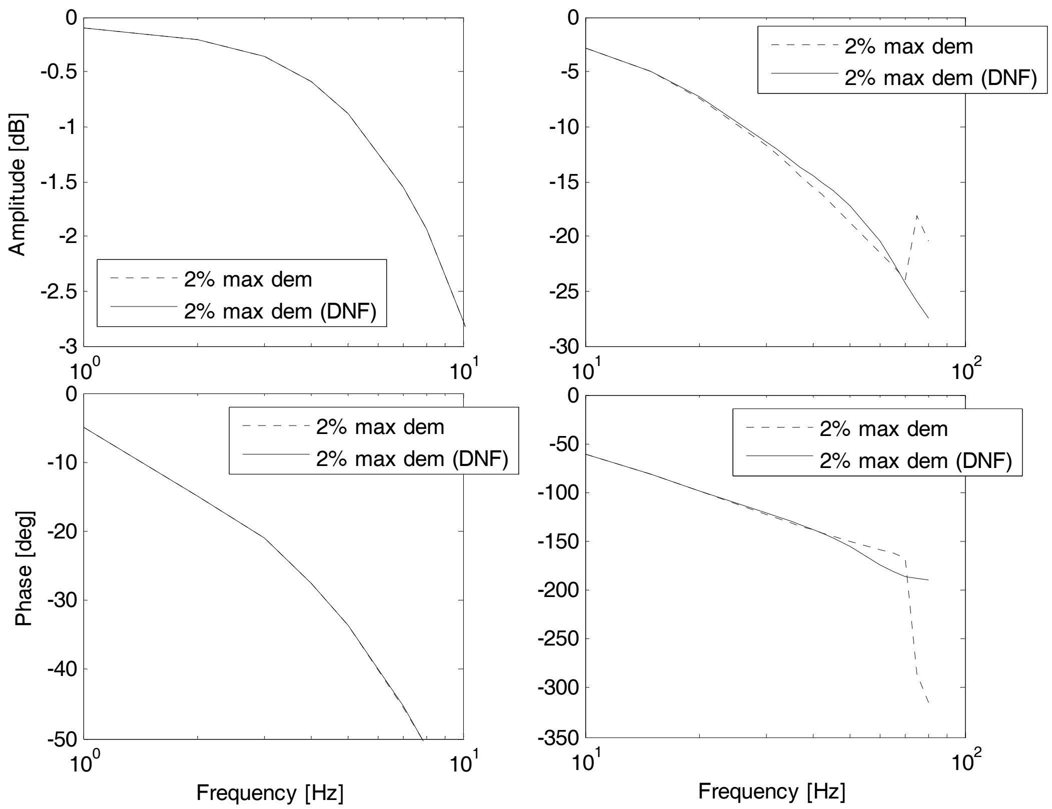

Fig. 7. Effects of the DNF on the actuator closed-loop dynamics (3 active coils).

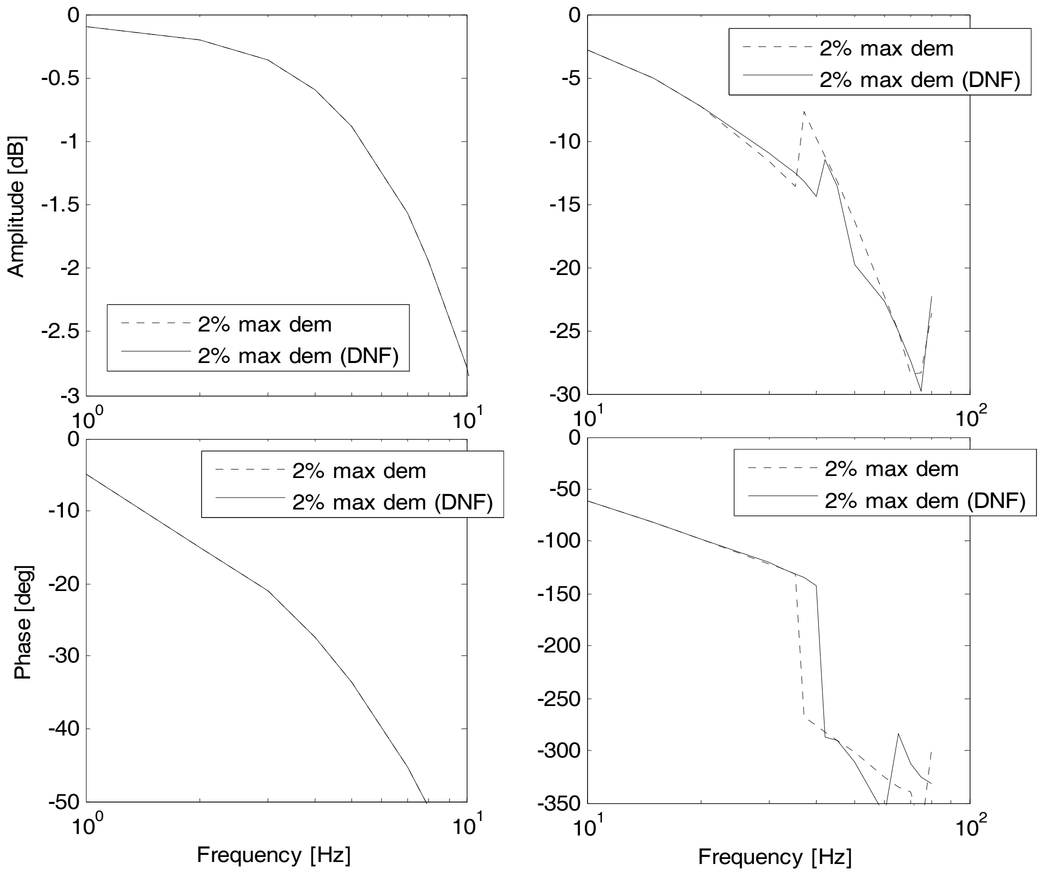

Fig. 8. Effects of the DNF on the actuator closed-loop dynamics (1 active coil).

Conclusion

A reconfiguration strategy for the closed-loop control of a fault-tolerant hydraulic actuator for fly-by-wire helicopters has been developed, demonstrating that the proposed technique is capable of compensating both servovalve coil failure effects and system nonlinearities.

The proposed approach combines a reconfiguration of the servovalve control gains with a dynamic notch filter (DNF) inserted in the servovalve closed-loop control, which essentially reduces the current demand when saturation conditions are achieved. The location of the DNF pulsation is obtained analytically, by modelling the actuator dynamics in case of current saturation, and by identifying the relationship between the actuator jump resonance frequency and the system dynamic characteristics. The effectiveness of the technique is assessed via simulation, by using an experimentally validated Matlab-Simulink model of the actuator developed by the authors. The actuator dynamics is characterised in terms of both servovalve and actuator frequency responses, with reference to the normal operative condition and with failures to the servovalve coils.

References

[1] Fielding C. *The design of fly-by-wire flight control systems*. BAE Systems Operations Limited, 2000.

[2] Collinson R P G. Fly-by-wire flight control. *Journal of Computing and Control Engineering*, pp. 141–152 1999.

[3] Webster F and Smith T D. *Flying qualities flight testing of digital flight control systems*. RTO-AG-300, Flight Test Techniques Series, Vol. 21, 2000.

[4] Pratt R W. *Flight control systems: practical issues in design and implementation*. The Institution of Electrical Engineers, 2000.

[5] Task Group SCI-026. *Flight Control Design – Best Practices*. RTO-TR-029, AC/323(SCI)TP/23, NATO Research and Technology Organization, 2000.

[6] Bonnice W F and Baker W. Intelligent fault diagnosis and failure management of flight control actuation systems. *NASA Contractor Report 177481*, 1988.

[7] Di Rito G, Galatolo R. Simulation and Experiments for the Study of a Fault-Tolerant Hydraulic Actuator for Fly-By-Wire Helicopters. *Proceedings of the 3rd CEAS Air&Space Conference-XXI Congresso Nazionale AIDAA*, Venice (Italy), pp. 1542-1551, 2011.

Contact Author Email Address

g.dirito@dia.unipi.it

Copyright Statement